

# Influence of processing conditions on geometrical features of laser claddings obtained by powder injection

J. M. PELLETIER, M. C. SAHOUR

GEMPPM-CALFETMAT, Bat. 502, INSA, 69621 Villeurbanne Cedex, France

M. PILLOZ

IUT, 12 rue de la Fonderie, 71200 Le Creusot, France

A. B. VANNES

MMP-CALFETMAT, ECL, BP 163, 69131 Ecully Cedex, France

The influence of processing conditions on the geometrical aspects of laser claddings is studied. Attention is drawn to the following laser-processing parameters: laser-power interaction time, surface of the irradiated zone, powder-feed rate. Different Ni–Cr–Co–Fe base powders are deposited on an austenitic stainless steel. It is observed that the mass of powder participating in the clad layer – which is proportional to the effective cross-section  $S$  of the layer – increases linearly with irradiance and interaction time. However, threshold values are detected; they are due to the existence of a minimum energy value required to melt the powder particles. The influence of the powder-feed rate,  $F$ , is more complicated. For low values,  $S$  is directly proportional to  $F$ , while beyond a critical value,  $F^*$ , the powder injected in the laser beam acts as a screen, the opacity of which increases due to the multiple scattering phenomenon; energy absorption is more and more efficient and process efficiency is enhanced. However, this increase is limited to a maximum value, since the energy delivered by the laser source is also limited and since cladding requires melting of the particles. A simple explanation is proposed, based on mass- and energy-transfer governing equations.

## 1. Introduction

A great deal of attention has been recently drawn to the possibilities of high-power lasers for surface alloying or cladding [1–6]. However, the main objective was often to achieve a precise application, especially to provide good tribological or electrochemical properties of materials and, usually, no systematic study of the influence of the different processing parameters was carried out. Such an investigation appears very useful for selecting the best combination of these variables. The present work will be focused on the influence of processing conditions on geometrical aspects of laser cladding and two classes of parameters can be distinguished.

1. materials parameters: thermal diffusivity,  $\alpha$ , and conductivity,  $k$ ; melting temperature,  $T_M$ , and latent heat of fusion,  $\Delta H_M$ ; specific heat,  $c$ ; density,  $\rho$ ; reflectivity,  $R$ , or its complementary value,  $A (= 1 - R)$ , at the wavelength of the laser,  $\lambda = 10.6 \mu\text{m}$ ; and, for powders, their granulometry: an average radius  $r_p$  is often defined.

2. laser processing parameters: laser power,  $P$ ; beam radius on the surface of the sample,  $r_b$ ; and laser-beam interaction time  $\tau$ .

All these parameters are not independent of each other and, in the present study, only the second group will be considered as variables. This will be illustrated by cladding experiments on a stainless steel; different powders have been chosen in order to deduce general features of the process.

## 2. Experimental procedure

The coating materials, Cenium 36 (Ce36), Metco 18C (M18C) and Metco 41C (M41C) alloy powders, which had the nominal compositions given in Table I, were sprayed with a Metco 4MP spray system, onto a grit-blasted stainless-steel substrate (304L). Specimens were mounted on a numerically controlled  $x$ - $y$  table and irradiated with a continuous  $\text{CO}_2$  laser, the power of which is up to 3.6 kW. The laser beam is focused by a spherical 10 inch Zn–Se lens. The scanning rate of the sample under the laser beam ( $v_T$ ) ranged from 3 to 15  $\text{mm s}^{-1}$ . A variation of the interaction time, defined by  $\tau = d/v_T$ , where  $d$  is the equivalent beam diameter on the sample, was thus possible. During scanning of the sample, argon was blown through a nozzle to prevent oxidation. No absorbing coating was used, to

TABLE I Nominal compositions of the different powders

| Powder | Composition (wt %) |    |      |      |     |   |     |    |   |    |
|--------|--------------------|----|------|------|-----|---|-----|----|---|----|
|        | Co                 | Cr | Ni   | Fe   | C   | W | Si  | Mn | B | Mo |
| M18C   | 40                 | 18 | 26.8 | 2.5  | 0.2 | — | 3.5 | —  | 3 | 6  |
| M41C   | —                  | 17 | 12   | 67.4 | 0.1 | — | 1   | —  | — | 6  |
| Ce36   | —                  | 30 | 36   | 20   | 1   | 5 | —   | —  | 3 | 9  |

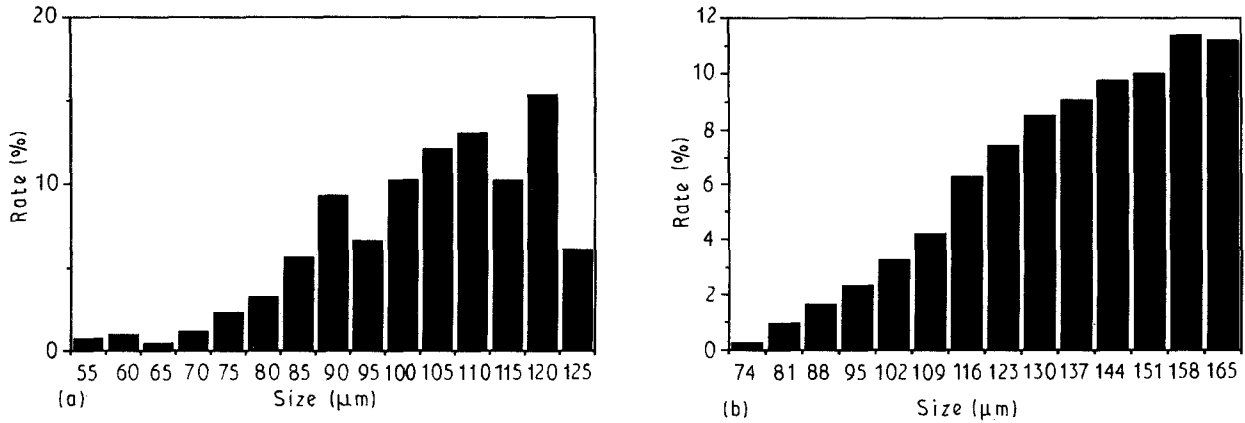


Figure 1 Size distributions of the different powders: (a) M18C and (b) M41C.

avoid contamination of the sample during melting. For optical-micrography and geometrical-feature determinations, samples were cut, polished and etched in the following reagent: 150 cm<sup>3</sup> HCl, 25 g K<sub>2</sub>Cr<sub>2</sub>O<sub>7</sub>, 50 cm<sup>3</sup> H<sub>2</sub>O.

Fig. 1 illustrates the size distribution of two different powders, as examples. A large range of diameters is covered.

### 3. Experimental results

#### 3.1. Optimization of the laser-processing conditions

The first stage of the optimization sequence is the determination of the range of the values of  $P$  and  $v_T$ , in which homogeneous and sound surface layers can be obtained, with a small dilution of the addition element into the substrate. This requires a very limited surface melting of this substrate. After various attempts, the following conditions were obtained:  $1000 < P < 2000$  W, and  $3.3 < v_T < 13.3$  mm s<sup>-1</sup>; the focus point was fixed 40 mm above the sample. Beam diameter at the impinging point is then  $2r_b \approx 1.5$  mm.

A typical cross-section of cladding is shown in Fig. 2. This cladding can be characterized by different parameters (Fig. 3): width  $L$ , thickness  $e$ , and surface  $S$  ( $\approx Le$ ) of this external part of the coating. (This value is therefore representative of the mass of powder participating in this clad region and, as  $L$  is nearly independent of  $P$  and  $v_T$ ,  $S$  will be retained as a pertinent parameter) and dilution rate, defined by:  $d\% = 100(e/e_T)$  where  $e_T$  is the total thickness of the area in which melting occurred, powder + substrate.

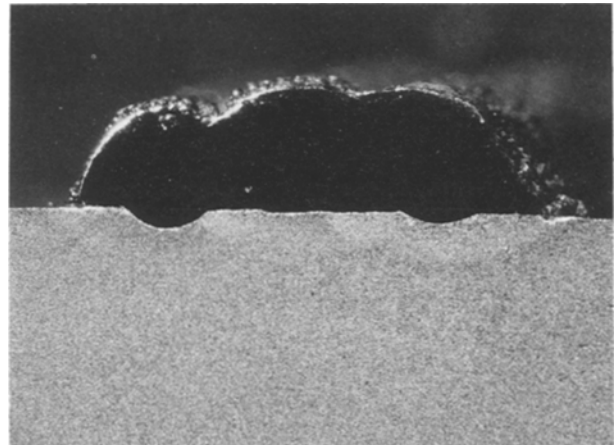


Figure 2 Typical micrograph of a laser cladding; powder; substrate 304L;  $P = 1600$  W;  $2r_b = 1.5$  mm;  $v_T = 6.6$  mm s<sup>-1</sup>,  $F = 30$  g min<sup>-1</sup> (G \*15).

#### 3.2. Influence of interaction time and laser power

Interaction time can be taken equal to  $\tau = 2r_b/v_T$ . Figs 4 and 5 show the combined influence of  $P$  and  $v_T$  for two different powders. These different results lead to the following conclusions:

1. For a given power value,  $P$ ,  $S$  increases linearly with interaction time, beyond a threshold value,  $\tau^*$ ; so this dependence can be written as  $S = m_1\tau + n_1$ , where  $m_1$  and  $n_1$  are constant values.

2. For a given value of  $\tau$ ,  $S$  also increases linearly with  $P$ . A threshold power is observed and then this variation is simply given by  $S = m_2P + n_2$ , where  $m_2$  and  $n_2$  are constant.

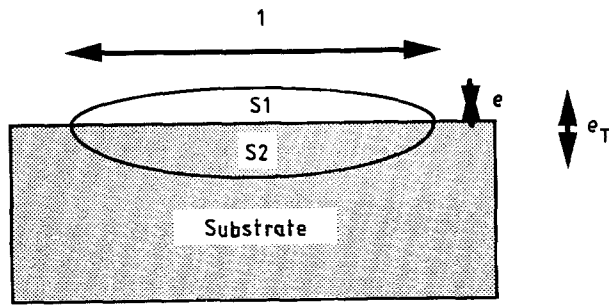


Figure 3 Schematic representation of a cross-section of a cladding.

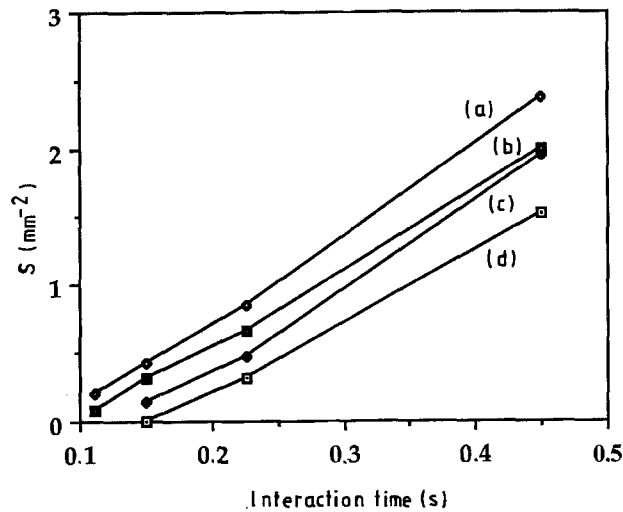


Figure 4 Influence of interaction time on the effective cross-section of the cladding (powder 18 C): (a) 2000 W, (b) 1600 W, (c) 1300 W, and (d) 1000 W.

### 3.3. Influence of powder feed rate

For a given laser power,  $P = 1500$  W, and a given interaction time,  $\tau = 0.45$  s, the effective cross-section is directly proportional to the feed rate ( $S = m_3 F$ ,  $m_3$  has a constant value) up to a critical value,  $F^*$  (Fig. 6). Beyond  $F^*$ , the increase is more pronounced. Values of  $m_3$  and  $F^*$  depend slightly on powder features. A metallographic investigation reveals that, for  $F > F^*$ , the dilution rates decrease more rapidly. A modification of the slope is observed at  $F^*$  (Fig. 7). So the melted part of the substrate becomes smaller and smaller and for feed rates higher than  $40 \text{ g min}^{-1}$ , the dilution rate is nearly negligible.

## 4. Discussion

The precise mechanism of laser cladding is very complicated [5, 6]. Indeed, in addition to the presence of two different materials, the melting phenomenon is complex since various possibilities (or even a combination of several ones) may be considered: (i) the powder melts during its transit between the nozzle and the specimen surface and then impinges onto the substrate and "pastes", inducing a partial melting of this region; (ii) the powder is only partially heated before impacting on the sample and melting occurs only during a further stage; (iii) the screen formed by the powder particles is not fully opaque and the

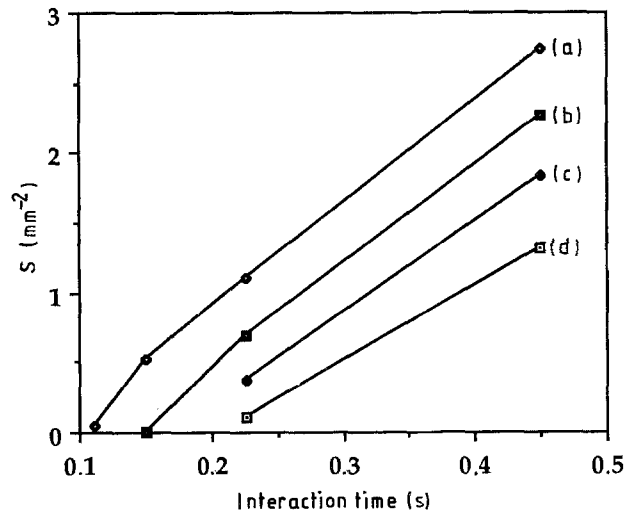


Figure 5 Influence of interaction time on the effective cross-section of the cladding (powder 41 C): (a) 2000 W, (b) 1600 W, (c) 1300 W, and (d) 1000 W.

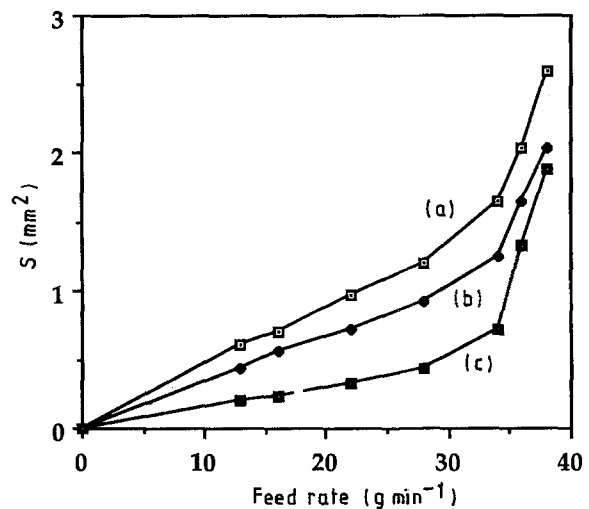


Figure 6 Influence of powder feed rate on the effective cross-section of the cladding: (a) M18C, (b) M41C, and (c) Ce36.

substrate melts before the arrival of the powder, especially if the melting point of this substrate is very low compared with the powder's (tungsten, carbides . . .) [7]; or (iv) powder is injected in the previously formed cladding and, due to the high scanning rate, this cladding is still liquid and incorporates the incoming particles, and a progressive building of this coating is then possible, without almost any participation of the substrate.

Any of these different possibilities can occur, depending on the materials under consideration and processing conditions; but in any case: (i)  $S$  is directly connected to the mass of powder participating in the clad layer, (ii) a minimum energy value is required to heat particles to their melting point, and (iii) the opacity of the powder screen has to be taken into account.

### 4.1. Influence of feed rate and interaction time on covering rate

If powder particles are assumed to be spheres with an

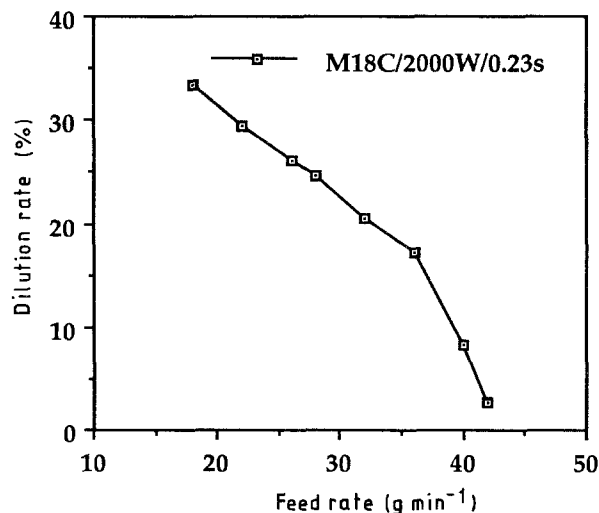


Figure 7 Influence of the powder feed rate on the dilution rate.

average radius,  $r_p$ , with a mass density,  $\rho$ , then the covering rate,  $C$ , can be defined as

$$C = n_1/n_2$$

where  $n_1$  is the number of incoming particles during the laser-material interaction time  $\tau$ , and  $n_2$  is the number of particles required to cover the entire surface of the laser-beam focusing area. Then this covering rate can be approximated by

$$C = \frac{3\gamma F\tau}{4\pi\rho r_p^2}$$

where  $F$  is the powder-feed rate and  $\gamma$  the powder efficiency, i.e. the ratio of the mass of powder participating in the clad layer to the mass of powder injected. This simple relationship is in agreement with the linear variations of  $S$  with both  $\tau$  and  $F$ , which have been experimentally observed (Figs 4–6). The existence of threshold values has now to be explained.

## 4.2. Energy statement

The minimum energy required to melt a mass,  $m$ , of material is given by

$$E^* = m(c\Delta\theta + \Delta H_M)$$

where  $\Delta\theta = T_M - T_0$  ( $T_M$ , melting temperature;  $T_0$ , initial temperature). In the present study, the main components of the powder are iron, cobalt, nickel and chromium. These transition elements have similar properties [8]. Then a first approximation can be obtained by taking the following average values  $\rho = 8 \text{ g cm}^{-3}$ ,  $c = 0.5 \text{ J g}^{-1}$ ,  $\Delta H_M = 250 \text{ J g}^{-1}$ ,  $T_M = 1500 \text{ }^\circ\text{C}$ .

So melting 1 g of material requires approximately 1000 J. Considering for example,  $F = 1 \text{ g s}^{-1}$  and  $P = 1000 \text{ W}$ , the minimum interaction time is then 1 s. However this value has to be modified, since two additional factors have to be taken into account.

1. The efficiency  $\gamma$  of the laser-cladding processing is lower than 100%. Indeed various limiting phenomena occur: the feeding system itself is not fully efficient; the powder flow cannot be perfectly localized

into the laser beam (divergence of the flow, difficulty of localization, etc); and some particles are heated, but not enough to reach their melting point and therefore cannot be incorporated in the cladding.

2. Part of the incident energy is reflected by the particles; this rate is characterized by the reflectivity.

Then the minimum energy becomes

$$E^* = 1000 F\gamma/(1 - R)$$

and, taking for example  $\gamma = 30\%$  and  $R = 50\%$ , we obtain  $E = 300 \text{ J}$  for a feed rate  $F = 30 \text{ g min}^{-1}$  ( $0.5 \text{ g s}^{-1}$ ). So, with an interaction time of 300 ms, a minimum laser power of 1000 W is required. A lower laser power would only induce heating of the additional material without melting and, consequently, without adhesion to the substrate and formation of an effective cladding. The existence of this threshold value of energy explains the existence of  $P^*$  values, in Figs 4 and 5.

## 4.3. Variation of the screen opacity

In order to explain the deviation from linearity shown in the curve of  $S$  versus  $F$  (Fig. 6), consider the mechanism of energy absorption within the powder cloud. When an energy  $E$  is incident on a material, it consists of three parts: a reflected energy  $ER$  (reflectivity) an absorbed energy  $EA$  (absorptivity  $A$ ), a transmitted energy  $ET$  (transmissivity  $T$ ).

For metallic materials, the transmitted value is usually negligible. In the present case this assumption appears realistic, since the average dimension of the powder particles is large enough (a few tens of micrometers). So,  $A + R = 1$ . When the powder-feed rate is low, the powder forms a dilute screen for the incident laser beam, which interacts only once with each particle. Whereas, a high feed rate induces a concentrated screen, within which each particle is submitted to a multiple scattering phenomenon (Fig. 8). A simple energy statement indicates that if the laser beam interacts  $n$  times with particles, the absorbed energy is no longer  $E(1 - R)$ , but  $E(1 - R^n)$ . Therefore the deviation from linearity observed in Fig. 6 could be attributed to a transition from a dilute screen to a concentrated screen, with the appearance of a multiple scattering phenomenon. This phenomenon leads to an increase in absorption and then to a better efficiency of the laser cladding process. This behaviour could be compared to percolation phenomena and is similar to light scattering across fog. This increase depends on particle size. Indeed, assuming a spherical shape for the particles (average radius  $r_p$ ), their number is, for a given feed rate  $F$ , proportional to  $r_p^{-3}$ , while the effective cross-section is proportional to  $r_p^2$ , leading to an interaction probability which varies as  $r_p^{-1}$ . Consequently, the smaller the particles are, the larger the screen opacity is. Notice that additional phenomena can occur for very small particles, i.e. when their size is smaller or equal to the wavelength of the laser beam ( $10.6 \mu\text{m}$  in the present study). Then Rayleigh scattering or interference could modify the interaction.

Fig. 9 summarizes the behaviour which may be predicted for the cladding rate. For a given powder

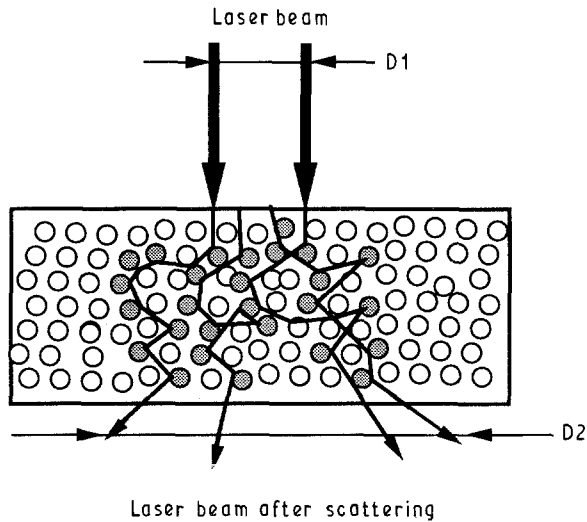


Figure 8 Multiple scattering phenomenon within the screen formed by the powder.

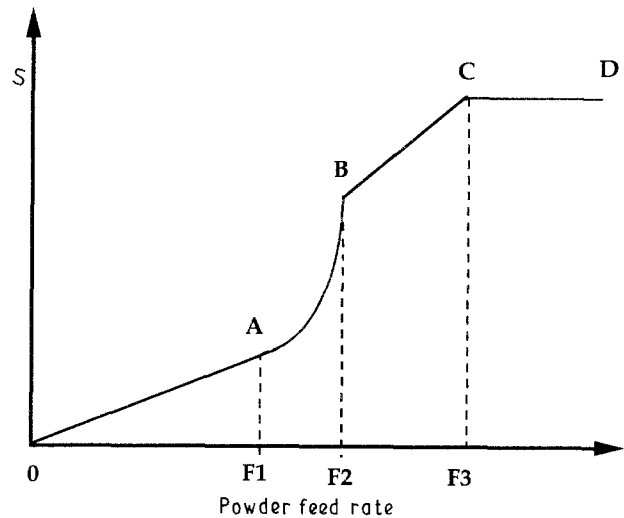


Figure 9 Schematic curve of the effective cross-section versus powder feed rate.

and for given laser processing conditions ( $P$ ,  $v_T$ ,  $r_b$ ), four different regions may be distinguished in the curve representative of the effective cross-section of the cladding versus the feed rate.

1. Part OA: powder screen is diluted, absorptivity of the laser beam by the particle flow is constant and therefore  $S$  increases linearly with  $F$ .

2. Part AB: screen opacity increases; the energy absorption also increases (to reach progressively  $A \approx 1$ ) and the cladding efficiency rapidly increases.

3. Part BC: screen is fully opaque, powder absorption is nearly equal to 1; the variation of  $S$  as a function of  $F$  is linear, for the second time; and the slope is higher than in part OA.

4. Part CD:  $S$  remains constant, since the incoming energy  $E$  enables melting of a given amount of matter; powder in excess is not melted and, therefore, is not added to the clad layer.

Values of  $F_1$  and  $F_2$  should depend on geometrical features of the powder, while  $F_3$  should depend on the chemical composition of the powder and on the energy delivered by the laser source.

## 5. Conclusion

A parametric study of the laser-cladding process by Ni-Co-Cr-Fe base-powder injection onto an austenitic stainless-steel substrate shows the following.

1. For given values of laser power and powder-feed rate, the mass of powder participating in the clad layer – which is proportional to the effective cross-section  $S$  of this layer – increases linearly with the interaction time.

2. For given values of interaction time and feed rate,  $S$  also increases linearly with the laser irradiance beyond a threshold value, which corresponds to the minimum energy required to melt the powder particles.

3. For given values of interaction time and laser irradiance, the influence of the feed rate  $F$  is more

complicated: in a first range  $S$  is directly proportional to  $F$ ; and beyond a critical value,  $F^*$ , the powder injected in the laser beam acts as a screen, the opacity of which increases, due to a multiple-scattering phenomenon. Energy absorption becomes more-and-more efficient and process efficiency is enhanced. However, this increase is limited to a maximum value, since the energy delivered by the laser source is also limited and since cladding requires melting of the particles.

A simple explanation is proposed, based on mass- and energy-transfer governing equations. Experimental results are in good agreement with the simple predictions of this model. Further experiments are in progress in order to confirm the present data, especially with different powders and different substrates.

## Acknowledgement

The authors appreciated the help provided by C. Vialle for the necessary experimental data.

## References

1. J. D. AYERS, *Thin Solid Films* **84** (1981) 223.
2. C. W. DRAPER, *J. Metals* **34** (1982) 24.
3. W. M. STEEN, in "Laser surface treatments of metals", edited by C. W. Draper and P. Mazzoldi, Martinus, Nijhoff, Dordrecht 1986, p. 369.
4. A. GALERIE, M. PONS and M. CAILLET, *Mat. Sci. Engng.* **88** (1987) 127.
5. J. SINGH and J. MAZUMDER, *Met. Trans.*, **18A** (1987) 313.
6. K. M. JASIM, R. D. RAWLINGS and D. R. F. WEST, *J. Mater. Sci.* **25** (1990) 4943.
7. P. KIRAT, F. FOUQUET, J. M. PELLETIER and A. B. VANNES, *Lasers Engng* **1** (1991) 67.
8. Y. S. TOULOUKIAN and D. P. DEWITT, in "Thermophysical properties of matter" (Plenum Press, New York, 1972).

Received 18 November 1991  
and accepted 20 August 1992